Critical behaviour of the bond-interacting self-avoiding walk

2007 J. Phys. A: Math. Theor. 40 1963

(http://iopscience.iop.org/1751-8121/40/9/004)

IOP Publishing Journal of Physics A: Mathematical and Theoretical

J. Phys. A: Math. Theor. **40** (2007) 1963–1980 doi:10.1088/1751-8113/40/9/004

Critical behaviour of the bond-interacting self-avoiding walk

D P Foster

Laboratoire de Physique Théorique et Modélisation (CNRS UMR 8089), Université de Cergy-Pontoise, 2 ave A. Chauvin 95035 Cergy-Pontoise cedex, France

Received 4 September 2006, in final form 15 December 2006
Published 14 February 2007
Online at stacks.iop.org/JPhysA/40/1963

Abstract

The phase diagram for the bond-interacting self-avoiding walk is calculated using transfer matrices on finite strips. The model is shown to have a richer phase diagram than the related Θ-point model. In addition to the standard collapse transition, we find a line of high-order phase transitions, which we conjecture to be in the Berezinskii–Kosterlitz–Thouless (BKT) universality class, terminating in a critical end point.

PACS numbers: 05.40.Fb, 05.20.+q, 05.50.+a, 36.20.−r, 64.60.−i

1. Introduction

Self-avoiding walk models are of interest both as models with which to understand the thermodynamic behaviour of polymers in solution, and as models of theoretical interest in their own right [1–3].

The thermodynamic behaviour of a linear polymer in dilute solution is determined by the competition between an attractive interaction, due to the difference between the monomer–monomer affinity and the monomer–solvent affinity, and an effective repulsive interaction (the excluded-volume interaction) which results from the loss in entropy caused by bringing together two segments of polymer. At high temperature the excluded-volume interaction dominates, leading to the good solvent phase, where the polymer adopts an open configuration, well interpenetrated by the solvent. At low temperatures the monomer–monomer affinity dominates and the polymer collapses into a dense ball, and in practice precipitates from solution. This is the bad solvent phase. These two phases are separated by the Θ-point transition [4, 5].

The thermodynamics of a polymer in solution is well modelled on the lattice by the so-called Θ-point model [6, 7], which consists of a self-avoiding walk on a regular lattice with the inclusion of attractive interactions between non-consecutively visited nearest-neighbour lattice sites. This model displays behaviour in excellent agreement with experimental results in both two and three dimensions. The critical behaviour of the 'on-lattice' model is in agreement

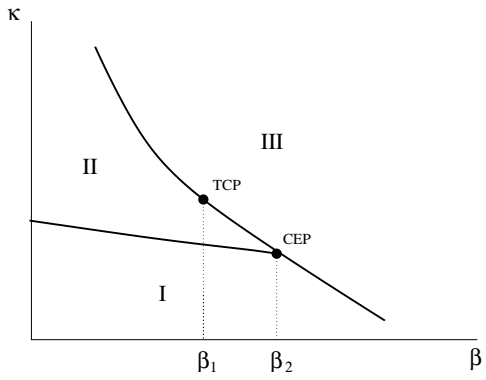

Figure 1. Phase diagram proposed by Stilck and co-workers [8, 9, 11]. The lower line is a critical line in the self-avoiding walk universality class, conjectured to terminate in a critical end point, CEP. The upper line is conjectured to be only made up of a critical transition line and a first-order transition line separated by a tricritical point, TCP. Phase I is the finite walk phase, phase II an isotropic dense phase, and phase III an anisotropic crystalline phase.

with the results of equivalent 'off-lattice' models, indicating that the lattice does not affect the critical behaviour.

The interesting feature of the Θ-point model is that it describes the thermodynamic behaviour of a large class of linear polymers, independently of the detailed chemistry of the polymer chain. This may be understood as follows: the real polymer chain, if long enough, behaves as a chain of spherical globules, comparable in size to the persistence length. The detailed chemistry simply defines the size of the globules, and the large-scale behaviour of the chain is described by a random walk, constrained by the excluded volume condition (globules repel each other due to entropic repulsion). The globules interact via effective attractive interactions, incorporating a variety of different microscopic interactions. The monomers in the model system then correspond to a large number of real monomers on the scale of the real polymer chain. Bearing this in mind, when going over to a lattice model, the decision to think of the 'monomers' sitting on the lattice sites or the lattice bonds is arbitrary. The choice of placing the interactions between the bonds would be, in principle, just as reasonable.

In this paper we present a transfer-matrix study of the bond-interacting self-avoiding walk model, and show that the phase diagram differs in many important ways from the standard Θ-point model, displaying richer behaviour. This model has been previously studied using extended mean-field-type calculations [8–10]. Different methods used by the different authors resulted in two different proposed phase diagrams. Support for the conjecture due to Stilck and co-workers [8, 9] (summarized in figure 1) is provided by Machado *et al* [11], who studied the model also using transfer-matrix methods. Our results differ in important details, and lend support to the phase diagram proposed by Buzano and Pretti [10]. This phase diagram is shown schematically in figure 2. We shall attempt to explain the reasons for these discrepancies.

2. The model and the transfer-matrix method

The model studied in this paper is the self-avoiding walk on the square lattice. A chemical potential μ, or equivalently a fugacity $\kappa = \exp(-\beta\mu)$, is associated with each step of the walk. An additional attractive energy $-\varepsilon$ is introduced every time two steps of the walk are

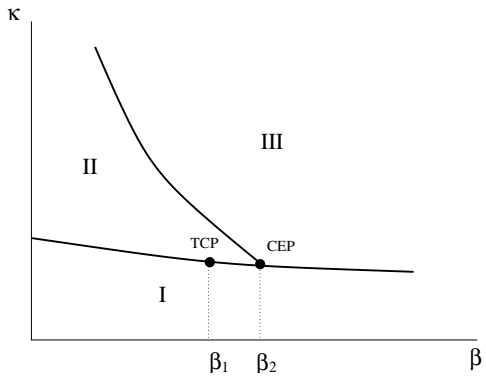

Figure 2. A conjectured schematic phase diagram, summarizing the results found in this paper. The phase diagram splits into three phases: (I) a finite walk phase ($\rho = 0$), (II) an isotropic dense walk phase (liquid phase) and (III) an anisotropic dense walk phase (crystalline phase). The transition from phase (I) to phase (II) is critical in the self-avoiding walk universality class for $\beta < \beta_1$ and first-order between β_1 and β_2 (in analogy with the standard Θ point model). The transition from phase (I) to phase (III) is first order. The transition occurring at β_1 is a tricritical point which we conjecture to be in the Θ universality class, whilst the transition at β_2 is a critical end point. The transition from phase (II) to phase (III) is conjectured to be in the BKT universality class.

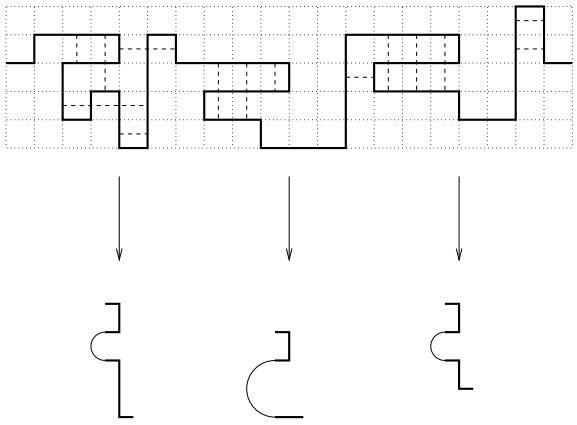

Figure 3. Example of a walk configuration, showing example column states. The nearest-neighbour interactions are indicated using dashed lines, whilst the thin lines show the connectivities that need to be taken into account in the column state.

parallel to each other across the face of a lattice plaquette, see figure 3. The thermodynamics of this model may then be studied in the grand-canonical ensemble by introducing the partition function:

$$\mathcal{Z} = \sum_{\text{walks}} \kappa^N \exp(N_I \beta \varepsilon), \tag{1}$$

where N is the number of steps in the walk, N_I is the number of interactions and $\beta = 1/kT$ as usual. It is convenient in what follows to set $\varepsilon = 1$, which is simply equivalent to a change in the temperature scale.

Once the partition function has been found, many thermodynamic quantities follow. The (dimensionless) free energy per site is defined as

$$f = \frac{\log \mathcal{Z}}{\Omega}, \tag{2}$$

where Ω denotes the number of sites on the lattice. The density, ρ, of the walk on the lattice and the energy per lattice site follow

$$\rho = \frac{\langle N \rangle}{\Omega} = \kappa \frac{\partial f}{\partial \kappa}, \tag{3}$$

$$e = \frac{E}{\Omega} = \frac{\langle N_I \rangle}{\Omega} = \frac{\partial f}{\partial \beta}. \tag{4}$$

Further derivatives give the response functions, the susceptibility and the specific heat.

In general there is no exact analytical result for the partition function, and so the thermodynamic quantities must be calculated either by simulation (for example using the Monte Carlo method) or some approximation scheme must be found enabling the determination of the partition function. In this paper we shall use the transfer-matrix method, where the exact partition function can be calculated for a lattice of finite width L and of infinite length [12–17]. The width of the lattice can then be varied, and the results extrapolated to infinite lattice width.

The standard way of considering the problem is as follows: define the restricted partition function $\mathcal{Z}_x(\mathcal{C}_0, \mathcal{C}_x)$ as the partition function for a portion of the lattice between $x = 0$ and x. The walk has a column state $\mathcal{C}_0$ at the origin and $\mathcal{C}_x$ in column x. One may then write the following recursion relation:

$$\mathcal{Z}_{x+1}(\mathcal{C}_0, \mathcal{C}_{x+1}) = \sum_{\mathcal{C}_x} \mathcal{Z}_x(\mathcal{C}_0, \mathcal{C}_x) \mathcal{T}(\mathcal{C}_x, \mathcal{C}_{x+1}), \tag{5}$$

where $\mathcal{T}(\mathcal{C}_x, \mathcal{C}_{x+1})$ is the additional Boltzmann weight to add column $x + 1$ in configuration $\mathcal{C}_{x+1}$ next to column x in configuration $\mathcal{C}_x$. This forms a (transfer) matrix.

That this recursion should be valid for a spin system is fairly straightforward, since the interactions are all local. For a polymer model it is less clear that this should be possible, since one has to take into account non-local factors, most notably to ensure that the partition function describes only one chain, without the formation of 'orphan' loops. This is done by appropriately defining the column states $\mathcal{C}_x$. For the self-avoiding walk problem with no added interactions (i.e., $\epsilon = 0$), it is sufficient to define a column configuration by the arrangement of horizontal bonds in the column along with information about the connectivities between the bonds [13–15], i.e. information about which pairs of horizontal bonds are connected by polymer loops to the left (taking x as increasing towards the right). See figure 3 for an example of how to define the column states for the bond-interacting model. By successive application of (5), one finds

$$\mathcal{Z}_x(\mathcal{C}_0, \mathcal{C}_x) = \langle \mathcal{C}_0 | \mathcal{T}^x | \mathcal{C}_x \rangle. \tag{6}$$

Since we are interested in equilibrium thermodynamic behaviour, and we shall be taking the limit $x \to \infty$, the choice of boundary conditions is arbitrary. Choosing periodic boundary conditions in the x direction results in $\mathcal{Z}_x = \mathrm{Tr}\ \mathcal{T}^x$, giving

$$\mathcal{Z}_x = \sum_i \lambda_i^x \tag{7}$$

terms of the eigenvalues λ_i of the transfer-matrix $\mathcal{T}$. In general the largest eigenvalue is non-degenerate, and the sum is dominated by this largest eigenvalue, λ_0, giving, in the limit $x \to \infty$,

$$f = \frac{1}{L} \log \lambda_0, \tag{8}$$

where L is the width of the lattice strip.

Having calculated the free energy, it is now possible to calculate the density, the energy and other local quantities by differentiation. However, since the eigenvalues of interest will be determined numerically, it is better to avoid differentiation whenever possible; the eigenvalues themselves may be calculated to arbitrary precision, but the numerical differentiation magnifies round-off errors, leading to a substantial loss of numerical precision. This is not a problem, however, since in the transfer-matrix framework it is easy to calculate averages over local quantities directly [18]. To see this, it is necessary first to calculate the probability of having a given configuration $\mathcal{C}_x$ in column x. This probability is simply the ratio of the partition function restricted to configuration $\mathcal{C}_x$ and the unrestricted partition function, which in terms of transfer matrices may be written as

$$p(\mathcal{C}_x) = \lim_{M\to\infty} \frac{\mathrm{Tr}\{T^x|\mathcal{C}_x\rangle\langle\mathcal{C}_x|T^{M-x}\}}{\mathrm{Tr}\, T^M}, \tag{9}$$

where M is the length of the lattice strip.

Writing $|\mathcal{C}_x\rangle$ in terms of the eigenvectors, $|i\rangle$ of $\mathcal{T}$ gives

$$p(\mathcal{C}) = \lim_{M\to\infty} \frac{\sum_i \lambda_i^M \langle i|\mathcal{C}\rangle\langle\mathcal{C}|i\rangle}{\sum_i \lambda_i^M} \tag{10}$$

$$p(\mathcal{C}) = \langle 0|\mathcal{C}\rangle^2, \tag{11}$$

where the eigenvectors are normalized. The subscript x may be omitted by invoking translation invariance.

The density, for example, is then found using

$$\begin{aligned}\rho &= \sum_{\mathcal{C}} \frac{N(\mathcal{C})}{L} p(\mathcal{C}) \\ &= \sum_{\mathcal{C}} \frac{N(\mathcal{C})}{L} \langle 0|\mathcal{C}\rangle^2,\end{aligned} \tag{12}$$

where $N(\mathcal{C})$ is the number of occupied lattice bonds in configuration $\mathcal{C}$. The susceptibility can then be calculated either by taking a derivative of the density, or by calculating directly $\langle N^2\rangle$ *for the column*, and hence the fluctuation. The two methods give slightly different results for a finite width strip, but agree in the thermodynamic limit. In the present paper we choose to calculate the fluctuation directly.

It is also possible to calculate two-point correlation functions, by considering the joint probability $p(\mathcal{C}_x, \mathcal{C}_y)$ of having a configuration $\mathcal{C}_x$ in column x and $\mathcal{C}_y$ in column y. The calculation proceeds exactly as above:

$$p(\mathcal{C}_x, \mathcal{C}_y) = \lim_{M\to\infty} \frac{\mathrm{Tr}\{\mathcal{T}^x|\mathcal{C}_x\rangle\langle\mathcal{C}_x|\mathcal{T}^{y-x}|\mathcal{C}_y\rangle\langle\mathcal{C}_y|\mathcal{T}^{M-y}\}}{\mathrm{Tr}\{\mathcal{T}^M\}} \tag{13}$$

$$= \lim_{M\to\infty} \frac{1}{\lambda_0^M} \langle\mathcal{C}_y|\mathcal{T}^{M+x-y}|\mathcal{C}_x\rangle\langle\mathcal{C}_x|\mathcal{T}^{y-x}|\mathcal{C}_y\rangle \tag{14}$$

$$\approx a + b\left(\frac{\lambda_0}{\lambda_1}\right)^{-(y-x)}, \tag{15}$$

where a and b are constants and λ_1 is the second largest eigenvalue. This leads directly to the identification of the correlation length as [19]

$$\xi = \frac{1}{\log\left(\frac{\lambda_0}{|\lambda_1|}\right)}. \tag{16}$$

The correlation length diverges when the two largest eigenvalues become degenerate, signalling the onset of a phase transition. For many spin models there is no phase transition below two dimensions, and so the correlation length should not diverge for finite lattice widths. In the transfer-matrix formulation this is seen explicitly by considering the Frobenious–Perron theorem, which states that for a finite-dimensioned matrix with strictly positive entries, the largest eigenvalue is non-degenerate [21]. In our model, however, there are many zero entries, and the Frobenious–Perron theorem does not apply. The potential degeneracy of the eigenvalues may be used to gain an insight into the phase diagram, and we shall return to this fact below.

The correlation length can be used as the basis of a phenomenological renormalization group analysis [22]. The idea is simple: far from the critical point the correlation length is smaller than the width of the lattice, but as the critical point is approached the divergence of ξ is limited by the smallest dimension, L. Since we expect to have scale invariance when both ξ and $L \to \infty$, all thermodynamic quantities should (for sufficiently large lattice sizes) be only a function of ξ/L. The critical point may then be identified with solutions of the equation:

$$\frac{\xi_L}{L} = \frac{\xi_{L'}}{L'}. \tag{17}$$

Two lattice sizes are required to determine the estimate, reducing the number of available estimates for extrapolation. There is no guarantee that there is a solution to this equation at finite lattice widths, and it is sometimes necessary to show that the gap goes to zero in the thermodynamic limit. Assuming the solution is an estimate for a phase transition, then using the asymptotic behaviour $\xi \sim |\kappa - \kappa_c|^{-\nu}$, we may infer estimates for ν at the same time:

$$\frac{1}{\nu_{L,L'}} = \frac{\log\left(\frac{\mathrm{d}\xi_L}{\mathrm{d}\kappa} \Big/ \frac{\mathrm{d}\xi_{L'}}{\mathrm{d}\kappa}\right)}{\log(L/L')} - 1. \tag{18}$$

Other quantities may be used in a phenomenological renormalization scheme. For self-avoiding walk type models the density is of particular interest. Close to a critical point the singular part of the free energy is expected to scale as

$$f_s(\kappa, L) = L^{-d}\tilde{f}(|\kappa - \kappa_c|L^{1/\nu}), \tag{19}$$

where d is the spatial dimension, here $d = 2$. Taking the first derivative with respect to κ gives

$$\rho_s = L^{1/\nu - 2}\tilde{\rho}(|\kappa - \kappa_c|L^{1/\nu}). \tag{20}$$

We have denoted the density as ρ_s since this is the density related to the singular part of the free energy, which vanishes in the thermodynamic limit. In general there will be a non-zero contribution from the non-singular part of the free energy, giving the limiting density. In walk models, the low-κ phase corresponds to finite length walks, and hence the density in the thermodynamic limit is zero. The scaling law then enables us to define a renormalization scheme [23, 24]. We start by defining the scaling function:

$$\varphi_{L,L'} = \frac{\log(\rho_s(\kappa, L)/\rho_s(\kappa, L'))}{\log(L/L'))}. \tag{21}$$

Since we wish to look for a family of estimators for the critical point, and taking into account that there are potentially severe parity effects, it is convenient to set $L' = L - 2$. Estimates of the critical point are then found by looking for solutions of the equation:

$$\varphi_{L,L-2}(\kappa_L^*) = \varphi_{L-2,L-4}(\kappa_L^*). \tag{22}$$

If such a solution exists, then $\kappa_c = \lim_{L\to\infty} \kappa_L^*$ and $\nu = \lim_{L\to\infty}(1/(2 + \varphi_{L,L-2}(\kappa_L^*))$.

Of course estimates of transition points can also be found by looking at appropriate susceptibilities, and identifying the transition with the peak of the function.

Each method has its advantages and disadvantages. The phenomenological renormalization group method proposed by Nightingale is usually the most asymptotic. However it is known that the dense self-avoiding walk is critical, and we could expect a high-κ critical phase. We shall argue here that the upper line found by Machado *et al* [11] is simply a particular critical line with in the critical dense-polymer phase, rather than the phase boundary as assumed. Caution is therefore important, and it is wise to cross-check results using different methods.

3. The κ–β phase diagram

In this section, the phase diagram is mapped out in the κ–β plane. A schematic phase diagram summarizing the mean-field results found by Buzano and Pretti [10] is shown in figure 2. Our results will tend to support this schematic phase diagram, and we refer to it in the following discussion.

It is expected that the model will have a behaviour similar to the Θ-point model as κ is increased from zero: at low enough κ the length of the walk is finite, and since the walk sits on an infinite lattice, the density is zero. The average length of the walk diverges along some line $\kappa = \kappa_1(\beta)$, either smoothly, for small enough β, or discontinuously, for large enough β. In the first case we have a critical phase transition in the same universality class as the self-avoiding walk model ($\beta = 0$) and in the second we have a first order transition. In the Θ point model the point separating the two regimes is a tricritical point, with a correlation length exponent $\nu = 4/7$, different from the self-avoiding walk value $\nu = 3/4$. Similarly, as β is increased along the line $\kappa = \kappa_1(\beta)$, the interactions of the bond-interacting self-avoiding walk will drive a collapse transition at some value of $\beta = \beta_1$.

In the Θ-point model there are no other phase transitions, in particular the whole high-κ phase is critical, believed to be in the same universality class as the dense self-avoiding walk [31]. In the bond-interacting model, whilst there is no direct energetic penalty to the formation of corners in the walk, in the dense phase the formation of corners reduce the number of possible interactions: two bonds forming a corner can have no facing bonds on the inside of the corner. This effect is much weaker than exists in similar models (such as the hydrogen-bonding model [12]), but, as the temperature is lowered, these interactions should drive a phase transition where the bonds making up the walk line up along one or other of the lattice directions. Extended mean-field calculations tend to confirm such a phase transition between two dense walk phases [8–10], an isotropic phase (the liquid phase II in figure 2) and an anisotropic phase (the crystalline phase III in figure 2). We will identify the transition line, $\kappa = \kappa_2(\beta)$, with a crystallization transition. This line will terminate on the line $\kappa = \kappa_1(\beta)$ at a value of $\beta = \beta_2$. An important question to be answered is whether $\beta_1 = \beta_2$, i.e., does the walk, as the line $\kappa = \kappa_1(\beta)$ is followed, collapse then crystallize, or rather collapse directly to a crystalline, anisotropic, state? The results we present in the next section tend to support the first scenario.

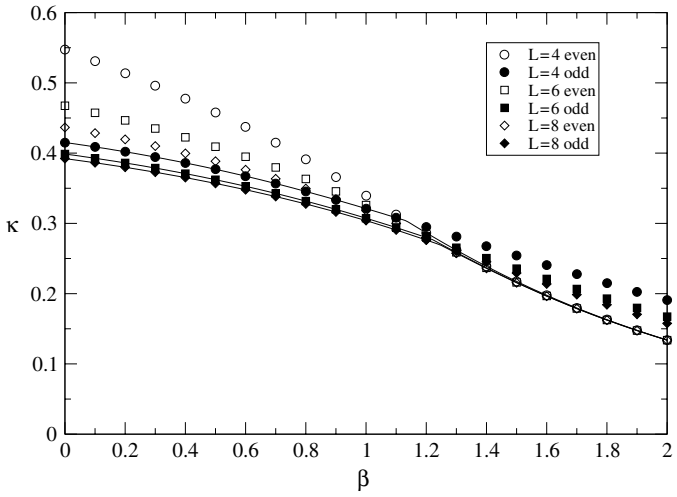

Figure 4. Estimates of the zero-density/finite-density phase transition line determined by setting $\lambda = 1$ for the even sector (open symbols) and odd sector (closed symbols). The solid lines indicate the transition line estimates. The collapse transition is identified with the point $\lambda_1 = \lambda_2 = 1$.

The transfer-matrix block diagonalizes naturally into three sectors: the vacuum state forms a block on its own, an odd sector (corresponding to walks with an odd number of links per column) and an even sector (where the walks have an even, non-zero, number of links per column).

In what follows, $\lambda_0 = 1$ is the eigenvalue corresponding to the vacuum state, λ_1 is the largest eigenvalue of the odd sector and λ_2 is the largest eigenvalue of the even sector.

We start by determining the transition line $\kappa_1(\beta)$. The transition line may be determined using the phenomenological renormalization group method with $\lambda_0 = 1$ in equation (16) [16]. This is shown in figure 6, along with phenomenological renormalization group estimates for $\kappa_2(\beta)$.

Alternatively, estimates may be obtained by setting $\lambda_1 = 1$ $(= \lambda_0)$. Since the smallest possible increase of density on a finite width lattice is $\Delta\rho = 1/L$, this transition, which exists at finite lattice widths, will appear as a first-order transition, becoming critical for $\beta < \beta_1$ in the infinite lattice width limit.

Whilst for the Θ-point model $\lambda_1 > \lambda_2$ everywhere, this is no longer true for the bond-interacting self-avoiding walk *for even lattice sizes*. For high enough β, λ_2 reaches one first as κ increases. Estimates of the $\kappa_1(\beta)$ transition line found by setting $\lambda_1 = 1$ and $\lambda_2 = 1$ are shown in figure 4. There is a point, then, on the $\kappa = \kappa_1(\beta)$ line in which we simultaneously have $\lambda_1 = \lambda_2 = 1$. By extension, the condition $\lambda_1 = \lambda_2$ defines a line in the κ–β plane. When $\lambda_1 = \lambda_2 < 1$, then the largest eigenvalue corresponds to the vacuum state $\lambda_0 = 1$. Crossings of subdominant eigenvalues indicate a change of local order, and define so-called disorder lines [25–28]. However, when $\lambda_1 = \lambda_2 > 1$ we have a crossing of the largest and second largest eigenvalues, and thus have a divergent correlation length. Since we expect phase II in figure 2 to be critical, we should not identify this line with the transition line $\kappa_2(\beta)$ without further evidence. The line must however indicate a change of order within the high-κ region of the phase diagram, and we argue below that this line plays the role of a critical 'disorder line', within the high-κ critical phase (II in figure 2). This line is shown in figure 6 along with

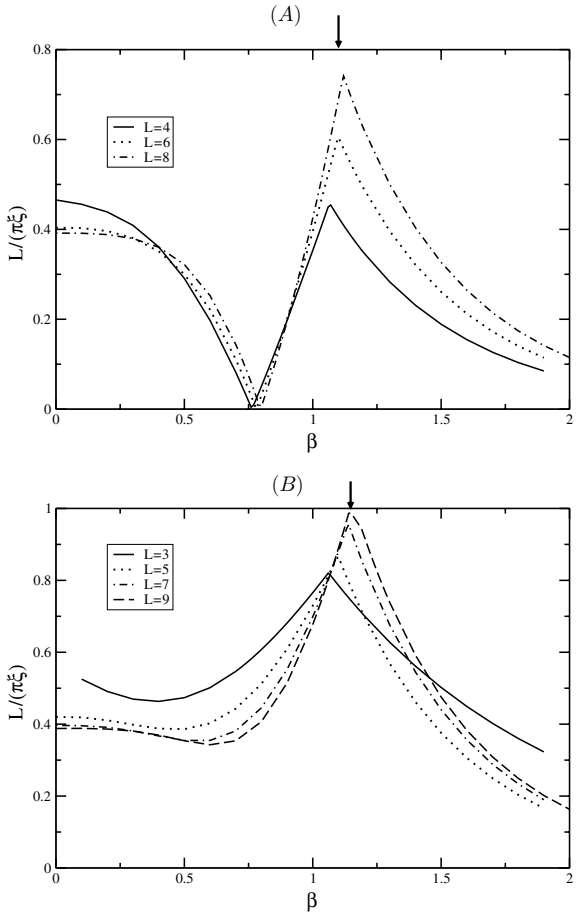

Figure 5. The combination $L/(\pi\xi)$ is plotted for different sizes as a function of β. The correlation function is calculated from the largest two eigenvalues. Up to the cusp (indicated by an arrow) the two largest eigenvalues come one each from the even and odd sector. Beyond the cusp the eigenvalues come from the same sector (even or odd depending on the parity of the lattice).

estimates of the phase boundaries. A disorder line cannot normally cross a critical line except at a special point, and so we tentatively identify the point $\lambda_1 = \lambda_2 = 1$ with the crystallization transition along the line $\kappa = \kappa_1(\beta)$. This identification is reasonable if one considers that in the crystalline phase the walk is trying to align its bonds with a lattice direction, so as to minimize the number of corners. For *even* lattice sizes the easiest way of achieving this is for the walk to fold back onto itself an even number of times. The corresponding configurations (when $\lambda_2 > \lambda_1$) sit in the even sector of the transfer matrix, leading to the observed crossover in the eigenvalues.

For critical points, conformal invariance arguments lead to the following relation for the correlation function exponent η [20]:

$$\eta = \frac{L}{\pi\xi}. \tag{23}$$

This combination is plotted in figure 5 separately for the even and odd lattice sizes in the high-κ region. We have calculated the correlation length using (16), where the eigenvalues are

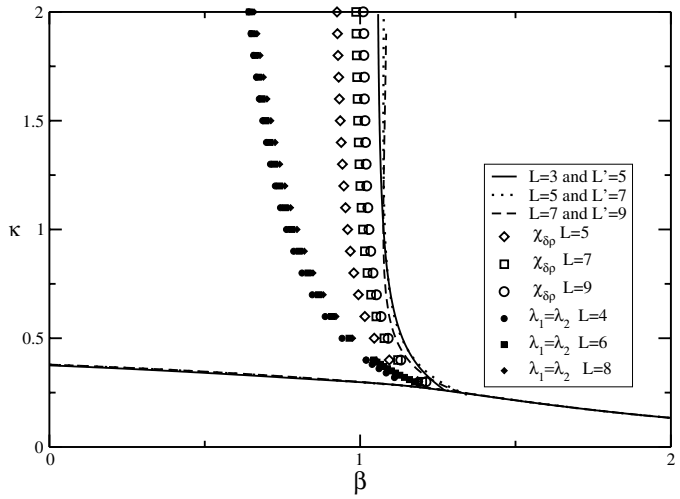

Figure 6. Proposed phase diagram calculated using the phenomenological renormalization group equation (17) using odd lattice widths. On the same diagram we plot the peaks of $\chi_{\delta\rho}$ which give an alternative estimate of the phase boundary. We also plot the solutions of $\lambda_1 = \lambda_2$ calculated for even lattice sizes.

the two largest eigenvalues of the full transfer matrix. In order to be sure of using the correct eigenvalues it is necessary to calculate the two largest eigenvalues of each sector. Up to the arrow indicated in the figure, the two largest eigenvalues correspond to the largest eigenvalue of each of the odd and even sectors. Beyond the arrow, the largest eigenvalues came from the same sector, either both even or both odd depending on the parity of the lattice. The different curves may clearly be seen to be collapsing onto a single curve for lower values of β, confirming the expectation of a critical phase. Close to the arrows, clear solutions to phenomenological renormalization group equation (17) may be seen, these are identified with the phase boundary, and plotted for odd lattice sizes in figure 6. The behaviour of the correlation lengths for even and odd lattice sizes agrees, and if plotted on the same graph (which, for clarity, we do not do here) can be seen to converge as the lattice size is increased.

It now remains to verify that the proposed phase boundaries do correspond to phase transitions, and if possible to say something about the nature of the phase transitions. With this in mind, it is natural to look for indicators such as response functions (fluctuations in the order parameter, specific heats, etc) which may be expected to show a singularity at the phase transition. A first step is to define a suitable order parameter. A good choice is the difference in densities of horizontal and vertical bonds, $\delta\rho = |\rho_h - \rho_v|$. The energy is maximized when all the monomers are parallel and pointing in the same direction. The effect of increasing temperature is to disorder this ground state, mixing up the two phases, and restoring isotropy. Figure 7 shows both $\delta\rho$, and corresponding fluctuations, for $\kappa = 0.5$, i.e. within the dense walk region of the phase diagram. The response function is $\chi_{\delta\rho} = L(\langle\delta\rho^2\rangle - \langle\delta\rho\rangle^2)$. Figure 8, on the other hand, shows the density and its corresponding fluctuations. The density of interactions and the density of corners have similar behaviour, excluding them as order parameters.

In figure 9 the specific heat is plotted for $\kappa = 0.5$, calculated directly from the grand-canonical free energy using the fluctuation-dissipation theory:

$$C_v = L\beta^2(\langle(e - \mu\rho)^2\rangle - \langle e - \mu\rho\rangle^2), \tag{24}$$

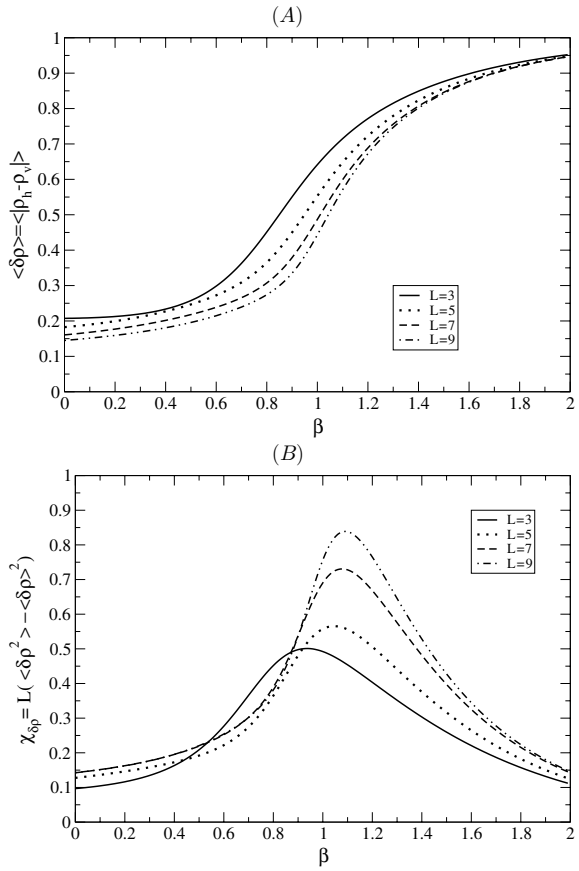

Figure 7. The order parameter, $\langle|\rho_h - \rho_v|\rangle$, suitable for the high-$\kappa$ transition (A) and its fluctuations (B) for $\kappa = 0.5$. Similar results are obtained for even lattice sizes.

where e is the energy per site and μ is the chemical potential ($\beta\mu = -\log\kappa$). The specific heat does not diverge, and has a broad peak, located at a lower value of β than the transition line for fixed κ, at a value of β consistent with the $\lambda_1 = \lambda_2$ line.

The evidence then points to the transition not being second order. We looked at the third and fourth order moments, and again found no sign of singular behaviour. The transition then seems to be a higher order transition between a critical high-temperature phase and an ordered low-temperature phase in which (almost) all corners are eliminated from the bulk. The ordered phase (III) has a density close or equal to 1. The transition is reminiscent of the transition found in the F-model (which is in the same class as the Berezinskii–Kosterlitz–Thouless (BKT) transition), which is an infinite-ordered phase transition, i.e. none of the derivatives of the free energy are singular. This identification is reinforced by the observation that the order parameter, $\delta\rho$, is not related to a derivative of the free energy. It is known that walk models with geometrically frustrated interactions can show this type of transition in the Hamiltonian walk limit $\kappa \to \infty$ [29]. To the best of our knowledge, this would be the first time this has been observed at finite κ. Clearly more work is required to verify this conjecture.

The phase diagram found in this section, and plotted in figure 6 is at odds with the phase diagram proposed by Machado *et al* [11]. Their proposed transition line was at a substantially

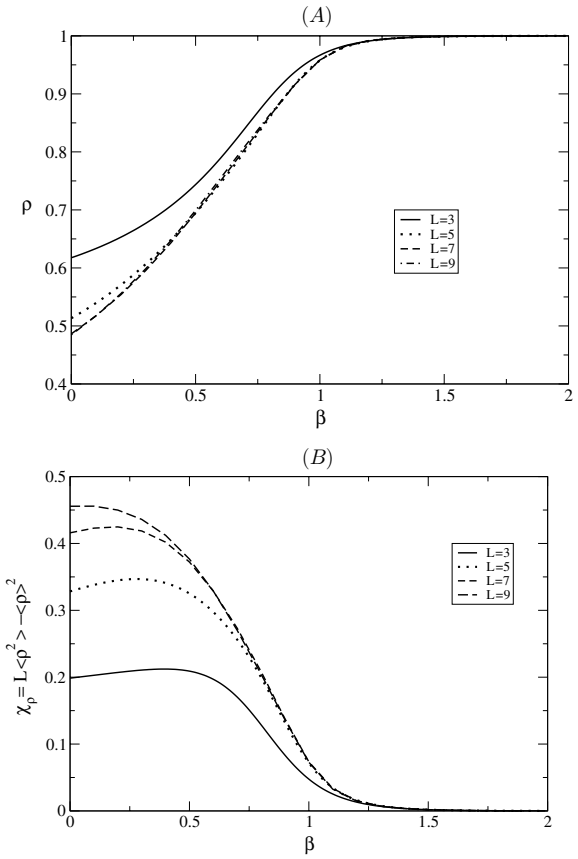

Figure 8. The density, ρ, (A) and its fluctuations (B) for $\kappa = 0.5$. The density of corners and the density of interactions behave similarly.

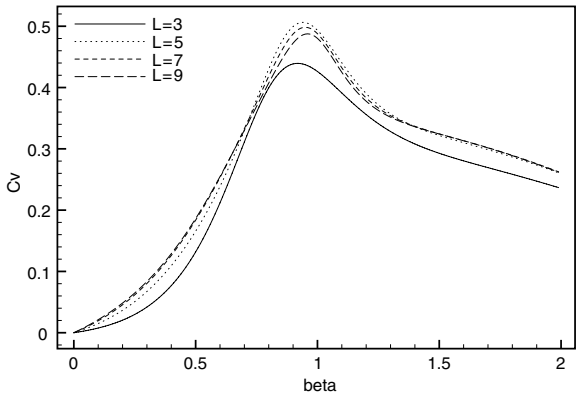

Figure 9. Plots for the specific heat for $\kappa = 0.5$. The peaks of the specific heat converge to a finite value, at a value of β lower than the phase transition.

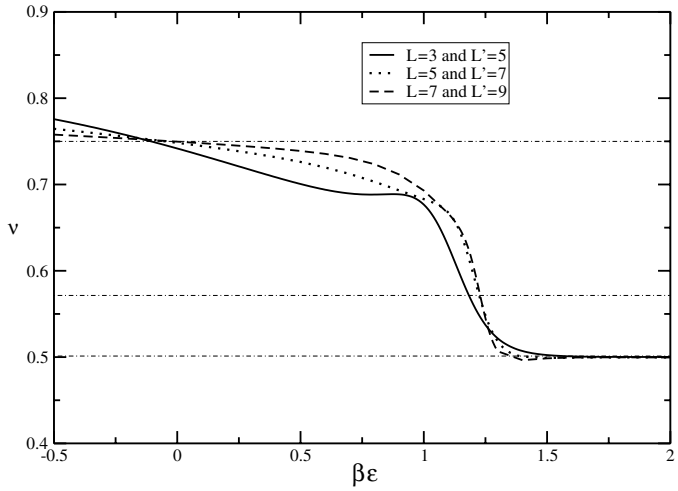

Figure 10. Estimates of ν calculated using (18). Using phenomenological renormalization arguments, crossings may be identified with fixed points. Dashed lines indicate the three special values of ν for the Θ-point model: $\nu_{\mathrm{SAW}} = 3/4$, $\nu_{\Theta} = 4/7$ and $\nu_{\mathrm{dense}} = 0.5$. We clearly see a fixed point corresponding to the pure self-avoiding walk model behaviour, as well as the correct dense walk limit as β is increased. Whilst the crossing between the $L = 3$, $L' = 5$ and the $L = 5$, $L' = 7$ line is far from $\nu = 4/7$, the crossing between the $L = 5$, $L' = 7$ and $L = 7$, $L' = 9$ lines is rather close. Unfortunately, with so few estimates, it is not possible to extrapolate. Note the possible appearance of an additional solution with $\nu \approx 2/3$, see text for discussion.

lower value of κ. They however limited their investigation to the odd sector of the transfer matrix, which restricts the configuration space available to walk. At first sight, this should not change the final results, since boundary conditions should not affect the bulk behaviour, *except for a critical phase*, where the correlation length diverges. We suggest that their method simply picks out a critical line within the critical phase II, and not, as assumed, the phase boundary. A similar analysis for the Θ-point model leads to a similar critical line, but here it is known that, whilst the high-density phase is critical, there is no phase transition.

4. Locating the multicritical points

In this section we shall try to pinpoint the location of the collapse transition and the crystallization transition along the $\kappa = \kappa_1(\beta)$ line in order to determine if these points are the same ($\beta_1 = \beta_2$), or if there are two distinct transitions ($\beta_1 \neq \beta_2$).

The most common way of locating the collapse transition is to plot ν estimates. For $T > T_{\mathrm{coll}}$, the collapse-transition temperature, the estimates tend to the self-avoiding walk value, whilst for $T < T_{\mathrm{coll}}$ the estimates of ν are expected to tend to $1/2$; as $\kappa \to \kappa^*$, the correlation length may be identified with the linear size occupied by the walk. Since, at the first order transition, the walk fills the lattice to a finite density, its linear dimension scales as $N^{1/2}$, or $|\kappa - \kappa^*|^{-1/2}$. The value of ν at the collapse transition is expected to take on an intermediate value. Crossings would be expected to converge to the point (β_{coll}, ν_{coll}) at the transition point. Additionally, (18) is simply a phenomenological renormalization group equation, and so crossings of ν may be identified with fixed points, corresponding to different universality classes.

Figure 10 shows the estimates for ν calculated using Nightingale phenomenological renormalization, see (18), for the odd lattice sizes, for which $\lambda_1 > \lambda_2$ along the whole line.

Table 1. Different estimates for the fugacity at the collapse transition, κ_{coll}, using the different methods described in the text.

L	Nightingale	φ	χ_ρ	$\chi_{\delta\rho}$	C_V	$\lambda_1 = \lambda_2 = 1$
3	0.268 701	0.258 766	0.377 05	0.304 06	0.314 15	–
4	0.280 168	0.270 168	0.348 15	0.354 43	0.357 81	0.303 687
5	0.277 469	0.267 450	0.311 16	0.267 44	0.280 73	–
6	–	–	0.270 17	0.302 31	0.314 40	0.277 016
7	–	–	0.288 71	0.259 80	0.272 25	–
8	–	–	0.285 16	0.278 86	0.295 73	0.269 245
9	–	–	0.280 02	0.258 72	0.269 49	–
∞			0.271 ± 0.003	0.258 ± 0.001	0.267 ± 0.001	

Table 2. Different estimates for the value of β at the collapse transition, β_{coll}, using the different methods discussed in the text.

L	Nightingale	φ	χ_ρ	$\chi_{\delta\rho}$	C_V	$\lambda_1 = \lambda_2 = 1$
3	1.283 504	1.283 169	0.679 46	1.089 35	1.042 56	–
4	1.205 824	1.205 822	0.776 46	0.942 86	0.930 14	1.133 416
5	1.240 191	1.240 300	0.987 83	1.240 91	1.172 57	–
6	–	–	1.038 50	1.138 37	1.055 22	1.220 231
7	–	–	1.114 07	1.278 27	1.213 09	–
8	–	–	1.139 36	1.203 15	1.122 13	1.2471 85
9	–	–	1.165 33	1.284 81	1.228 18	–
∞			1.23 ± 0.02	1.29 ± 0.01	1.24 ± 0.01	

The estimates may clearly be seen to cross. There is also an intriguing series of shoulders, which seem to accumulate to form a fixed point with a value of $\nu \approx 2/3$, close to the branched polymer value for ν [30]. This may be an indication that the walk forms branching structures before fully collapsing. This is more likely to be a crossover effect than a true phase transition, but this point warrants further investigation.

The values calculated for the crossing points are given in tables 1 and 2. With so few data points it is not possible to extrapolate, particularly remembering that there are strong parity effects, however, looking at the odd lattice sizes, the transition is likely to be in the region of $\beta_{\text{coll}} \approx 1.22$–$1.24$. Values of ν are consistent with a collapse transition in the Θ-point universality class ($\nu_{3,5,7} = 0.525\,974$, $\nu_{5,7,9} = 0.556\,653$ and $\nu_\Theta = 4/7 = 0.571\,4286$).

The location of the collapse transition can be estimated from the peaks of the response function for the corresponding order parameter. The density provides a good order parameter for the collapse transition, whilst $\delta\rho$ provides a good order parameter for the crystallization transition. The plots of χ_ρ and $\chi_{\delta\rho}$ along the transition line are given in figure 11, and the location of the corresponding peaks is given in tables 1 and 2. The results derived from $\chi_{\delta\rho}$ indicate a transition which is certainly at a value of $\beta > 1.27$ whilst χ_ρ indicates that the collapse transition occurs at a value of $\beta < 1.25$. This leads to the conclusion that there are at least two distinct multicritical points along the low-κ transition line ($\kappa = \kappa_1(\beta)$).

We cross-check these results using additional estimates for the transition points. For the collapse transition we used phenomenological renormalization using ρ (see (20)–(22)), whilst for the crystallization transition we looked for solutions to $\lambda_1 = \lambda_2 = 1$. Plots of $\varphi_{L,L+2}$ are shown in figure 12 and the estimates for the transition points using these two methods are, again, shown in tables 1 and 2. The estimates for ν found using the phenomenological renormalization group are again consistent with a Θ-point transition.

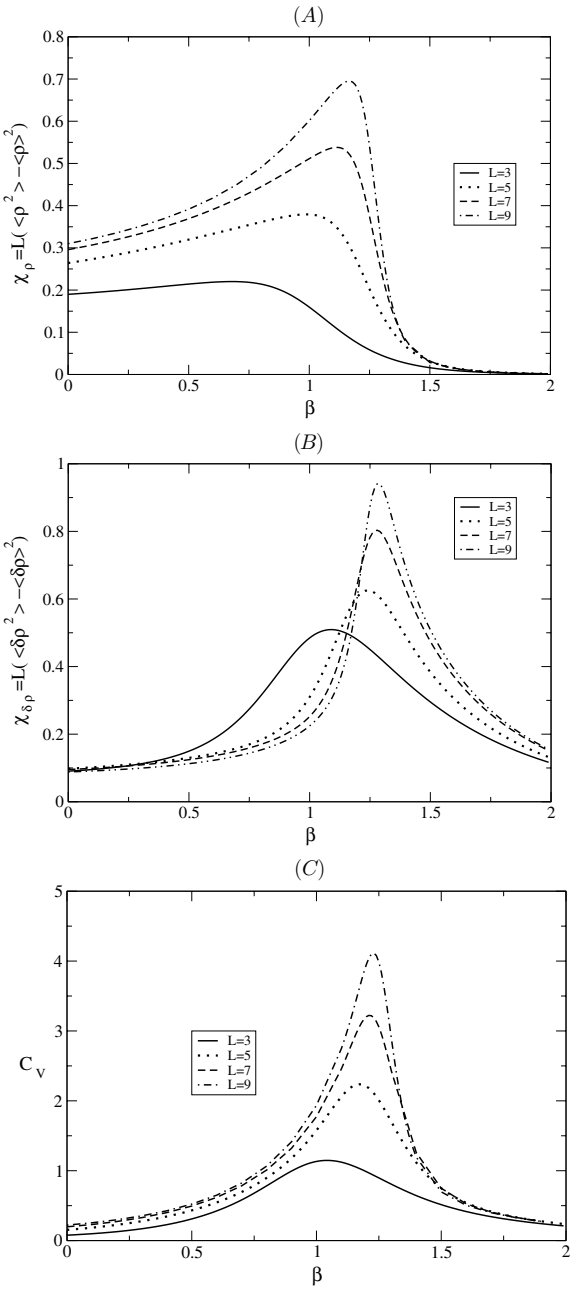

Figure 11. Plots of (*A*) χ_ρ, (*B*) $\chi_{\delta\rho}$ and (*C*) the specific heat with $\kappa = \kappa^*\beta$, along the low-κ-transition line.

5. Discussion

There are two basic phase diagrams proposed in the literature for this model, both based on extended mean-field-type calculations. By the mean-field nature of the calculations, they can only propose general features, and not details of critical behaviour. This is amplified in

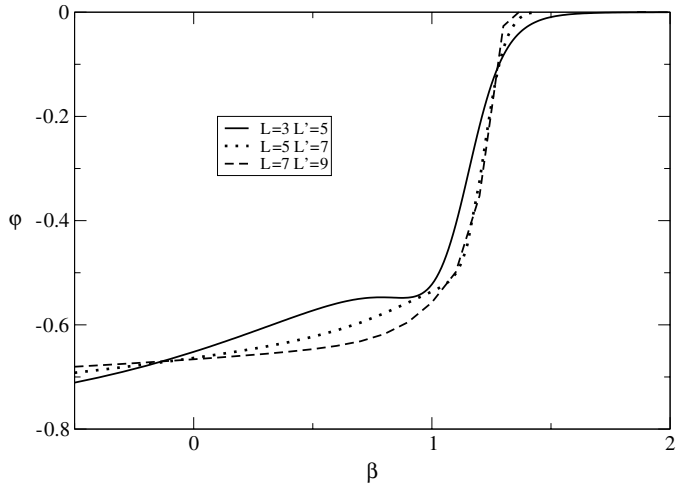

Figure 12. $\varphi_{L,L+2}(\beta)$ plotted along the low-κ-transition line. Again we see crossings corresponding to the self-avoiding walk fixed point, and the collapse transition. For the Θ point we would expect a value of $\varphi = -1/4$. From the above figure the estimate of φ is closer to -0.11 ($\nu \approx 0.53$), although the value of φ does decrease as L is increased. Again with just two solutions, it is not possible to extrapolate.

walk models, since the connectivities, and thus the single walk nature of the model, cannot be taken into account in the local description inherent in the methods used. However, our transfer-matrix calculations tend to confirm the qualitative predictions made by Buzano and Pretti [10] rather than those made by [8, 9]. In summary, we propose the phase diagram shown qualitatively in figure 2. Moving along the self-avoiding walk line, the walk first collapses by the standard Θ-point type transition, followed by a further transition where the corners are ejected from the walk, and the walk lines up with one of the two lattice directions. This latter transition is similar to the transition seen in the so-called F-model of a gas of semi-rigid self-avoiding loops filling the lattice with a density equal to 1 ($\kappa \to \infty$). In the F-model the transition is in the BKT universality class. We have found evidence that the bond-interacting self-avoiding walk model may also display a BKT transition, but unusually this transition is extended into a line of transitions in the high-κ phase. This point requires further work.

Whilst the Θ-point model does not show a dense walk phase transition, other models do, notably the hydrogen-bonding self-avoiding walk model [12], the Blöte–Nienhuis $O(n)$ walk model [31] and the Θ-point model with the inclusion of a bending interaction [10, 32–35]. These models all have one feature in common: they include interactions which are geometrically frustrated. It is expected that this frustration is seen when the density of the walk becomes finite, where the fractal (or Hausdorff) dimension is equal to the lattice dimension [23]. In the bond-interacting model the exponent ν found for the collapse transition is clearly larger than $1/2$, hence the Hausdorff dimension is lower than the lattice dimension, and we could therefore expect the critical behaviour not to be modified by any lattice effects. In this case it is reasonable to expect the collapse transition to be in the Θ universality class.

It is interesting to note that in the three models in which the dense-phase transition line has been studied beyond mean field, i.e. the Blöte–Nienhuis $O(n)$ model, the hydrogen-bonding model and the bond-interacting model, all seem to have different classes of transition: for the Blöte–Nienhuis $O(n)$ model the dense-phase transition line was in the Ising universality class [36], in the hydrogen model the transition was critical with a divergent specific heat with

a value of $\nu < 1$ [23] and now the bond-interacting model with transition of order higher than four (possibly a BKT transition). At first sight it seems as if there are as many different thermodynamic behaviours as models one might define, but preliminary results for a hydrogen-bonding self-avoiding walk, extended to include solvent quality effects (in the language of a polymer model) indicate that this model displays at least the latter two behaviours [37].

Whilst transfer-matrix calculations enable an exploration of the whole phase space, not accessible to Monte Carlo simulation, the method is hampered by the small number of lattice widths available. Recently we introduced an extension to the CTMRG method for walk models [23, 24], but unfortunately this method is not easy to implement for bond interactions. Monte Carlo simulation may be useful to study the limit $N \to \infty$, enabling an independent study of the different transitions proposed.

Acknowledgments

The author would like to thank C Pinettes for useful discussions and a careful rereading of the manuscript.

References

[1] de Gennes P G 1979 *Scaling Concepts in Polymer Physics* (Ithaca: Cornell University Press)
[2] des Cloiseaux J and Jannink G 1990 *Polymers in Solution: Their Modelling and Structure* (Oxford: Oxford University Press)
[3] Vanderzande C 1998 *Lattice Models of Polymers* (Cambridge: Cambridge University Press)
[4] Flory P J 1971 *Principles of Polymer Chemistry* (Ithaca: Cornell University Press)
[5] de Gennes P G 1972 *Phys. Lett.* A **38** 339
[6] Domb C 1974 *Polymer* **15** 259
[7] Wall F T and Mazur J 1961 *Ann. NY Acad. Sci.* **89** 573
[8] Stilck J F, Machado K D and Serra P 1996 *Phys. Rev. Lett.* **76** 2734–7
[9] Serra P, Stilck J F, Cavalcanti W L and Machado K D 2004 *Journal Phys. A: Math. Gen.* **37** 8811–21 http://stacks.iop.org/0305-4470/37/8811
[10] Buzano C and Pretti M 2002 *J. Chem. Phys.* **117** 10360
[11] Machado K D, de Oliveira M J and Stilck J F 2001 *Phys. Rev.* E **64** 051810
[12] Foster D P and Seno F 2001 *J. Phys. A: Math. Gen.* **34** 9939–57 http://stacks.iop.org/0305-4470/34/9939
[13] Klein D J 1980 *J. Stat. Phys.* **23** 561
[14] Enting I G 1980 *J. Phys. A: Math. Gen.* **13** 3713
[15] Derrida B 1981 *J. Phys. A: Math. Gen.* **14** L5
[16] Derrida B and Saleur H 1985 *J. Phys. A: Math. Gen.* **18** L1075–9 http://stacks.iop.org/0305-4470/18/L1075
[17] Derrida B and Herrmann H J 1983 *J. Phys. France* **44** 1365
[18] Foster D P, Gérard C and Puha I 2001 *J. Phys. A: Math. Gen.* **34** 5183–200 http://stacks.iop.org/0305-4470/34/5183
[19] Yeomans J M 1992 *Statistical Mechanics of Phase Transitions* (Oxford: Oxford University Press)
[20] Cardy J L 1984 *J. Phys. A: Math. Gen.* **17** L385
[21] Horn R and Johnson C 1990 *Matrix Analysis* (Cambridge: Cambridge University Press)
[22] Nightingale M P 1976 *Physica* A **83** 561
[23] Foster D P and Pinettes C 2003 *J. Phys. A: Math. Gen.* **36** 10279–98 http://stacks.iop.org/0305-4470/36/10279
[24] Foster D P and Pinettes C 2003 *Phys. Rev.* E **67** 045105
[25] Stephenson J 1970 *J. Math. Phys.* **11** 420
[26] Stephenson J 1970 *Can J. Phys.* **48** 2118
[27] Stephenson J 1970 *Can J. Phys.* **48** 1724
[28] Stephenson J 1969 *Can J. Phys.* **47** 2621
[29] Saleur H 1986 *J. Phys. A: Math. Gen.* **19** 2409–23 http://stacks.iop.org/0305-4470/19/2409
[30] Parisi G and Sourlas N 1981 *Phys. Rev. Lett.* **46** 871
[31] Blöte H W J and Nienhuis B 1989 *J. Phys. A: Math. Gen.* **22** 1415

[32] Lise S, Maritan A and Pelizzola A 1998 *Phys. Rev.* E **58** R5241–R5244
[33] Bastolla U and Grassberger P 1997 *J. Stat. Phys.* **89** 1061
[34] Doniach S, Garel T and Orland H 1996 *J. Chem. Phys.* **105** 1601–8
[35] Doye J P K, Sear R P and Frenkel D 1998 *J. Chem. Phys.* **108** 2134–42
[36] Guo W, Blöte H W J and Nienhuis B 1999 *Int. J. Mod. Phys.* C **10** 301
[37] Foster D P and Pinettes C in preparation